Developmental Biology 357 (2011) 518–531

Contents lists available at ScienceDirect

Developmental Biology

journal homepage: www.elsevier.com/developmentalbiology

Genomes and Developmental Control

Identification of an evolutionarily conserved regulatory element of the zebrafish *col2a1a* gene

Rodney M. Dale, Jacek Topczewski *

Northwestern University, Feinberg School of Medicine, Department of Pediatrics, Children's Memorial Research Center, 2300 Children's Plaza, Box 204, Chicago, IL, 60614, USA

ARTICLE INFO

Article history:
Received for publication 14 April 2011
Revised 3 June 2011
Accepted 16 June 2011
Available online 25 June 2011

Keywords:
Collagen
Cranial sutures
Growth plate
Intervertebral disc
Semicircular canals
Weberian apparatus

ABSTRACT

Zebrafish (*Danio rerio*) is an excellent model organism for the study of vertebrate development including skeletogenesis. Studies of mammalian cartilage formation were greatly advanced through the use of a cartilage specific regulatory element of the *Collagen type II alpha 1* (*Col2a1*) gene. In an effort to isolate such an element in zebrafish, we compared the expression of two *col2a1* homologues and found that expression of *col2a1b*, a previously uncharacterized zebrafish homologue, only partially overlaps with *col2a1a*. We focused our analysis on *col2a1a*, as it is expressed in both the stacked chondrocytes and the perichondrium. By comparing the genomic sequence surrounding the predicted transcriptional start site of *col2a1a* among several species of teleosts we identified a small highly conserved sequence (R2) located 1.7 kb upstream of the presumptive transcriptional initiation site. Interestingly, neither the sequence nor location of this element is conserved between teleost and mammalian *Col2a1*. We generated transient and stable transgenic lines with just the R2 element or the entire 1.7 kb fragment 5′ of the transcriptional initiation site. The identified regulatory elements enable the tracking of cellular development in various tissues by driving robust reporter expression in craniofacial cartilage, ear, notochord, floor plate, hypochord and fins in a pattern similar to the expression of endogenous *col2a1a*. Using a reporter gene driven by the R2 regulatory element, we analyzed the morphogenesis of the notochord sheath cells as they withdraw from the stack of initially uniform cells and encase the inflating vacuolated notochord cells. Finally, we show that like endogenous *col2a1a*, craniofacial expression of these reporter constructs depends on Sox9a transcription factor activity. At the same time, notochord expression is maintained after Sox9a knockdown, suggesting that other factors can activate expression through the identified regulatory element in this tissue.

Introduction

Collagens are a major component of the extracellular matrix in all metazoans and therefore are one of the most abundant proteins expressed in the animal kingdom (Exposito et al., 2010; Prockop and Kivirikko, 1995). The evolution of the fibrillar collagens is also associated with the evolution of the notochord, the defining characteristic of chordates (Wada et al., 2006). The advent of the notochord, a cartilaginous rod-like structure derived from the axial mesoderm, allowed early chordates to have rigid structured tails necessary for efficient swimming (Wada et al., 2006). Complex genetic networks evolved to direct the formation of skeletal elements associated with the notochord, such as vertebrae, ribs, and neural arches. These structures provide mechanical support for various types of locomotion, form the appendages, and protect the internal organs. Formation of these skeletal elements require cartilage molds made of chondrocytes expressing Type II Collagen, one of the most abundant and well studied of the fibrillar collagens.

The expression pattern of *col2a1* is conserved from teleosts to mammals and is observed in the developing cartilage, notochord, skin, floor plate, brain, and heart, among other tissues (Cheah et al., 1991; Kerney et al., 2010; Yan et al., 1995; Zhou et al., 1995). Congenital defects caused by mutations in the *col2a1* gene, known as Type II collagenopathies, vary in severity and include abnormal skeletal growth and density, early onset of osteoarthritis, and retinal detachment (Boot-Handford and Tuckwell, 2003; Hoornaert et al., 2010; McAlinden et al., 2008; Miyamoto et al., 2005; Spranger et al., 1994). The distinct and conserved expression pattern of the *col2a1* gene and the identification of a small regulatory element within the first intron of mice and humans make it an excellent marker and genetic tool to study cartilage and skeletal development in mammals (Zhou et al., 1995).

The zebrafish is an excellent genetic model for the study of skeletal cartilage and notochord formation (Crump et al., 2006; Dutton et al., 2008; Halpern et al., 1997; Renn et al., 2006). With the optically transparent body of the zebrafish embryo and larva, tissue specific expression of fluorescent proteins is an especially fruitful method to

* Corresponding author at: Children's Memorial Research Center, Room C421F, 2300 Children's Plaza, Box 204, Chicago, IL 60614-4314, USA. Fax: +1 773 755 6385.
E-mail addresses: r-dale@northwestern.edu (R.M. Dale), j-topczewski@northwestern.edu (J. Topczewski).

0012-1606/$ – see front matter © 2011 Elsevier Inc. All rights reserved.
doi:10.1016/j.ydbio.2011.06.020

investigate morphogenetic movements of cells. Most of the currently available regulatory elements used to drive expression in cranial chondrocytes are targeted for expression in the precursor cells, the multipotent cranial neural crest (Dutton et al., 2008; Lawson and Weinstein, 2002). As a result, multiple other cell types are labeled at the stage of skeletogenesis. While the expression of *col2a1a* in zebrafish is an excellent marker for the development of cartilage and the notochord, a zebrafish regulatory element able to specifically drive expression in *col2a1a* expressing tissues has yet to be identified.

In this study we set out to identify the zebrafish *col2a1a* regulatory element that will allow for targeted gene expression in chondrocytes and other domains of its expression. Since the zebrafish has two homologues of *col2a1*, the intensively characterized *col2a1a* (Yan et al., 1995) and the previously uncharacterized *col2a1b*, we first compared their expression patterns through the early stages of development to determine whether either was expressed in the chondrocytes. We found that only *col2a1a* is robustly expressed in all craniofacial chondrocytes and, thus, has cartilage regulatory element(s) driving cartilage expression. Using a teleost-based comparative genomics approach, we identified a small, novel, and highly conserved regulatory element upstream of the *col2a1a* gene. This element with a minimal promoter is able to drive expression in the cranial and postcranial cartilages, ear, and the notochord. The relatively small size of this regulatory element makes it easy to manipulate and drive targeted gene expression. Using reporter constructs based on the *col2a1a* regulatory element we were able to track the cellular behavior during notochord development, in particular the formation of notochord sheath cell layer from the initially uniform stack of notochord cells. Additionally, knockdown of *sox9a*, a gene known to regulate *col2a1a* expression, reduces the reporter expression driven by this regulatory element in the cranial cartilages, but not in the forming ear or notochord.

Materials and methods

In silico analysis

Genomic and protein sequences for both *col2a1a* and *col2a1b* were obtained from the NCBI and Wellcome Trust Sanger databases for multiple vertebrates. Genomic synteny was determined by pair-wise multialignments of teleost genomes of fugu (*Takifugu rubripes*), tetraodon (*Tetraodon nigroviridis*), medaka (*Oryzias latipes*), stickleback (*Gasterosteus aculeatus*), and zebrafish (*Danio rerio*) obtained from the Wellcome Trust Sanger Ensembl database comparing the two neighboring genes on either side of *col2a1* homologues. Identified conserved genomic synteny was further confirmed using the Synteny Database (Catchen et al., 2009). The automatic prediction was complicated by the fact that the Ensembl database of *col2a1* homologues lists zebrafish *col2a1a* as 1 of 2 and *col2a1b* as 2 of 2, while the other teleost *col2a1b* is listed as 1 of 2 leading misrepresentation of the synteny relation.

These genomic sequences around the 5′ end of the *col2a1a* gene were compared using the mVISTA program (http://genome.lbl.gov/vista/index.shtml) for regions of 100% homology over a 10 nucleotide window.

Protein sequences of Col2a1 homologues were obtained from NCBI and aligned and compared using the MultiAlin software (http://multalin.toulouse.inra.fr/multalin/multalin.html) using a Blosum62 comparison table (Corpet, 1988).

In situ hybridization

The *col2a1a* anti-sense RNA probe was synthesized from previously described plasmid, (ZDB-GENE-980526-192) (Yan et al., 1995) with T3 RNA polymerase. The zebrafish *col2a1b* was identified using bioinformatics methods and a cDNA clone pCMV-Col2a1b (accession# BC059180) was obtained from Open Biosystems. A fragment of the *col2a1b* plasmid was subcloned into the pBlueScript vector to remove its polyA tail. The *col2a1b* anti-sense RNA probe was synthesized with T7 RNA polymerase from a HincII cut of the pBS-*col2a1b* plasmid. Whole mount *in situ* hybridization was performed as described in Sisson and Topczewski(2009) and Thisse(2000) using high stringency conditions (65% formamide hybridization buffer with a 0.05% SSC final wash).

Plasmid construction and Gateway recombineering

Plasmids were made using the Multistep Gateway Recombineering system (Invitrogen) and the Tol2kit (Kawakami and Shima, 1999; Kwan et al., 2007) to generate transgenic fish. Using the primers listed below, the appropriate *att* recombineering sites were added to flank the targeted genomic sequences for proper pDONR integration. Fragments were amplified, purified and incubated with the BP enzyme and pDONR vectors overnight. Desired clones were selected and propagated. The promoter entry vectors were then mixed with the proper reporter gene, pDestTol2pA2 vector and LR enzyme and incubated overnight.

Promoter element	Forward primer	Reverse primer
R1	ATAACCCATGCCCTACTGATGACC	AGTGTCACCATACACACATGGAGC
R2	CCTCTGACACCTGATGCCAATTGC	AGGGATATGTGTATGTGTGTGTACGC
−116 (R3)	GTGGTGGACTTCTTTCCCAATGG	TTGCAGGTCCTAAGGGGTGAAAGTCG
−389 (R3)	GACTGTACACTGTATGCATAAGGACC	TTGCAGGTCCTAAGGGGTGAAAGTCG
R4	TTCAGTGTGTGTGAGGGCTGTCC	GTCTGCGTATTTGAAACTGAACCC
−1.7 kb	CCTCTGACACCTGATGCCAATTGC	TTGCAGGTCCTAAGGGGTGAAAGTCG

Microinjection and screen of regulatory elements

Wild type fish were injected at the 1–2 cell stage with 5–10 pg of the desired plasmid. Injected embryos were transferred to 1× egg water and incubated at 28 °C for 24 h. Embryos were then screened under a Zeiss SteREO Discovery.V8 fluorescent microscope for EGFP or mCherry expression and imaged using either a Zeiss AxioPlan2 compound microscope or a Zeiss LSM 510 META confocal.

Generation of stable transgenic lines

Embryos were injected with either the *−1.7kbcol2a1a:EGFP-CAAX* or the *R2-E1b:EGFP* plasmids at the 1–2 cell stage then screened at 24 h post fertilization (hpf) for the presence of EGFP. Positive embryos were selected and grown to adulthood. These embryos were then out crossed with AB wild type fish lines. Progeny from this cross were then screened for the presence of EGFP to identify stable transgenic founders. We identified 3 independent insertions of the −1.7kb*col2a1a:EGFP-CAAX*, referred to as Tg(*1.7c2a1a:mGFP*)^{nu12}, ^{nu17}, ^{nu18} and 3 independent insertions of the *R2-E1b:EGFP*, referred to as Tg(*R2c2a1a:GFP*)^{nu13}, ^{nu14}, ^{nu16}. No difference was observed between the insertions in the reporter expression pattern for both constructs except for one line, Tg(*1.7c2a1a:mGFP*)^{nu17}, which has expression in the same tissues as the other lines but at a much lower level and mosaically.

Microinjection and screen of regulatory elements and sox9a morpholino

Tg(*1.7c2a1a:mGFP*)^{nu12} or *Tg*(*R2c2a1a:GFP*)^{nu13} fish were crossed with AB wild type fish and progeny were injected at the 1–2 cell stage with 2–5 ng of *sox9a* morpholino (Open Biosystems, (Yan et al., 2002). Injected and uninjected embryos were transferred to 1× egg water and incubated at 28 °C for 24 h. Embryos were then screened under a fluorescent microscope for EGFP expression in the notochord. Positive embryos for EGFP were cultured and further analyzed using a Zeiss LSM 700 confocal and then separated for further imaging at 4 days

post fertilization (dpf) for scoring of cartilage, ear, and fin EGFP expression.

Zebrafish husbandry

The *Tg*(*Bactin:HRAS-EGFP*)^{vu119} (ZDB-GENO-061107-1), wild-type, and stable transgenic fish lines created during this work were maintained as described in LeClair et al.(2009). Embryos were collected from natural spawning and staged according to morphology as described in Kimmel et al. (1995). Standard length (SL) staging described by Parichy et al. (2009) was used for fish older than 4 days post-fertilization (dpf). The value of measurements of SL reflects better the progress of development than age of the animal. All images are marked with the actual distance from the snout to the caudal peduncle in millimeters (mm), except for Fig. 3E where eye diameter was used to calculate SL. The fish protocols and care in this paper were approved by the IACUC of Children's Memorial Research Center (Chicago, IL), an AALAC-accredited facility.

Live and fixed embryo confocal imaging

Transgenic embryos were fixed in 4% PFA overnight at the designated days post-fertilization (dpf) and then extensively washed in PBS with 0.01% Triton-X100 (PBT). Embryos were then stained with Alexa Fluor 647 conjugated Wheat Germ Agglutinin (Invitrogen) at a ratio of 1:150 overnight at 4 °C and again washed with PBT then stained with DAPI at a ratio of 1:1000 for up to 2 h at room temperature then washed with PBT. Embryos were mounted in 50% glycerol on a glass slide. The vital bone staining was done using the Alizarin red protocol as described (Kimmel et al., 2010). Live embryos were anesthetized in a 0.15% tricane solution in egg water then mounted in a 1% low-melt agarose 0.15% tricane solution in transplantation buffer, 0.3× modified Niu Twitty buffer with HEPES (Niu and Twitty, 1953). Embryos were imaged either on a Zeiss LSM 510 META or LSM 700 laser confocal microscope. Time-lapse of laser confocal z-stack images were captured every 12 min for up to 16 h.

Cryosections

Following whole mount *in situ* hybridizations, embryos were post-fixed with 4% paraformaldehyde, mounted in sucrose agar blocks, frozen, and cut into 10 μm sections. Sections were analyzed and imaged on a Zeiss Axioplan II microscope using the AxioVision 4.8 software (Zeiss).

3D reconstruction and movie generation

A time-lapse movie was generated using the LSM 700 confocal microscope and Zen confocal imaging processing software (Zeiss). Z-stack images were collected approximately every 12 min for 16 h. To generate 3D images and movies, two z-stacks per hour were chosen and inputted into the AMIRA 5.3 3D rendering software (Visage Imaging). Individual *1.7c2a1a:mCherry* and mGFP labeled cells were outlined for each z-stack over time and rendered. The rendered images were then put together in a time-series to generate a 3D rendered movie.

Results

Two teleost col2a1 homologues have distinct genomic synteny

The main goal of this work was the isolation of genetic elements capable of cartilage specific expression at embryonic, larval and adult stages of zebrafish development. In tetrapods, only one *collagen type II, alpha 1* (*col2a1*) gene has been described (Cheah et al., 1985, 1991; Kerney and Hanken, 2008). A conserved mammalian enhancer first identified in mouse (Zhou et al., 1995) within the *col2a1* gene is widely used in skeletal biology studies (Han and Lefebvre, 2008; Hattori et al., 2008; Zhang et al., 2006b). Interestingly, agnathans such as lamprey and hagfish have two *col2a1* homologues suggesting that multiple homologues of *col2a1* existed early in the vertebrate lineage (Ota and Kuratani, 2010; Zhang et al., 2006a). We searched zebrafish genomic databases and found only two genes, *col2a1a* (Yan et al., 1995) and *col2a1b* a second homologue, that had been identified but not characterized (Woods et al., 2005). Furthermore, we determined that two *col2a1* homologues are similarly present in the tetraodon, fugu, medaka, and stickleback genomes (Figs. 1A,B). We found upon inspection of the genomic region around each of the *col2a1* teleost homologues that there is a high degree of conserved genomic synteny (Figs. 1A,B). Only in zebrafish are the genes located downstream of *col2a1a* in other fish species found on a different chromosome, suggesting a translocation event occurred after separation of the zebrafish lineage from other fish.

The genomic synteny around the human *COL2A1* gene, located on chromosome 12, and other tetrapods has been well documented (Morvan-Dubois et al., 2003). Interestingly, the presence of zebrafish *col2a1b* and multiple other genes on the distal end of chromosome 11 was used as evidence of a common origin of this region with human chromosome 12 (Woods et al., 2005); however, most of the genes conserved around the fish *col2a1b* found on human chromosome 12 are at least 10 megabases away from human *Col2a1*. This suggests that either extensive chromosomal remodeling has taken place in this region during mammalian evolution or that this linkage is random.

When compared to human COL2A1, the zebrafish Col2a1a and Col2a1b proteins are highly conserved as they share greater than 70% identity at the amino acid level (Supplemental Fig. 1A) (Exposito et al., 2010). Comparison of the Col2a1 sequences of multiple teleost, amphibian, and mammalian species revealed that the teleost Col2a1b group is more similar to the Col2a1 of mammals and amphibians than the teleost Col2a1a (Fig. 1C).

Expression domains of col2a1a and col2a1b partially overlap in the developing zebrafish embryo

We predicted that a second zebrafish homologue of *col2a1* could have similar cartilage specific expression. If this were correct, a detailed sequence alignment of the two paralogues' promoters could reveal a shared cartilage specific regulatory unit. To compare the expression patterns of the very well characterized zebrafish *col2a1a* (Yan et al., 1995) with the uncharacterized *col2a1b*, we performed whole mount *in situ* hybridization on zebrafish embryos from the 3 somite stage through 4 days post-fertilization (dpf) (Figs. 1D–O). Expression of both transcripts was first detected at the 3 somite stage, at the midline of the embryo, marking the forming notochord (Supplemental Figs. 1B,D). By mid-segmentation, *col2a1a* is strongly expressed in the floor plate, notochord, hypochord, and the axial endoderm, with faint expression in the mesenchymal cells of the head (Figs. 1D,E). In contrast, *col2a1b* is expressed in the notochord with weak expression in the floor plate, ear, and mesenchymal cells of the head (Figs. 1F,G). Unlike *col2a1a,* no expression of *col2a1b* was observed in the hypochord (Fig. 1F). By 24 h post-fertilization (hpf), the early pharyngula stages, *col2a1a* expression in the floor plate, hypochord, and head is maintained, while the *col2a1a* expression in the vacuolated notochord cells is gradually lost in an anterior to posterior fashion (Fig. 1H). At this stage, expression of *col2a1b* is almost absent in the trunk and tail region, with the exception of the most posterior tip of the notochord, but is beginning to be upregulated in the head mesenchyme (Fig. 1I). Expression of *col2a1b* in the individual epidermal cells becomes visible at this stage (Fig. 1I). On the second day of development, we observed non-neuronal *col2a1b* expression at the level of the midbrain–hindbrain boundary and the forming olfactory pits (Supplemental Figs. 1C,E). Both domains are

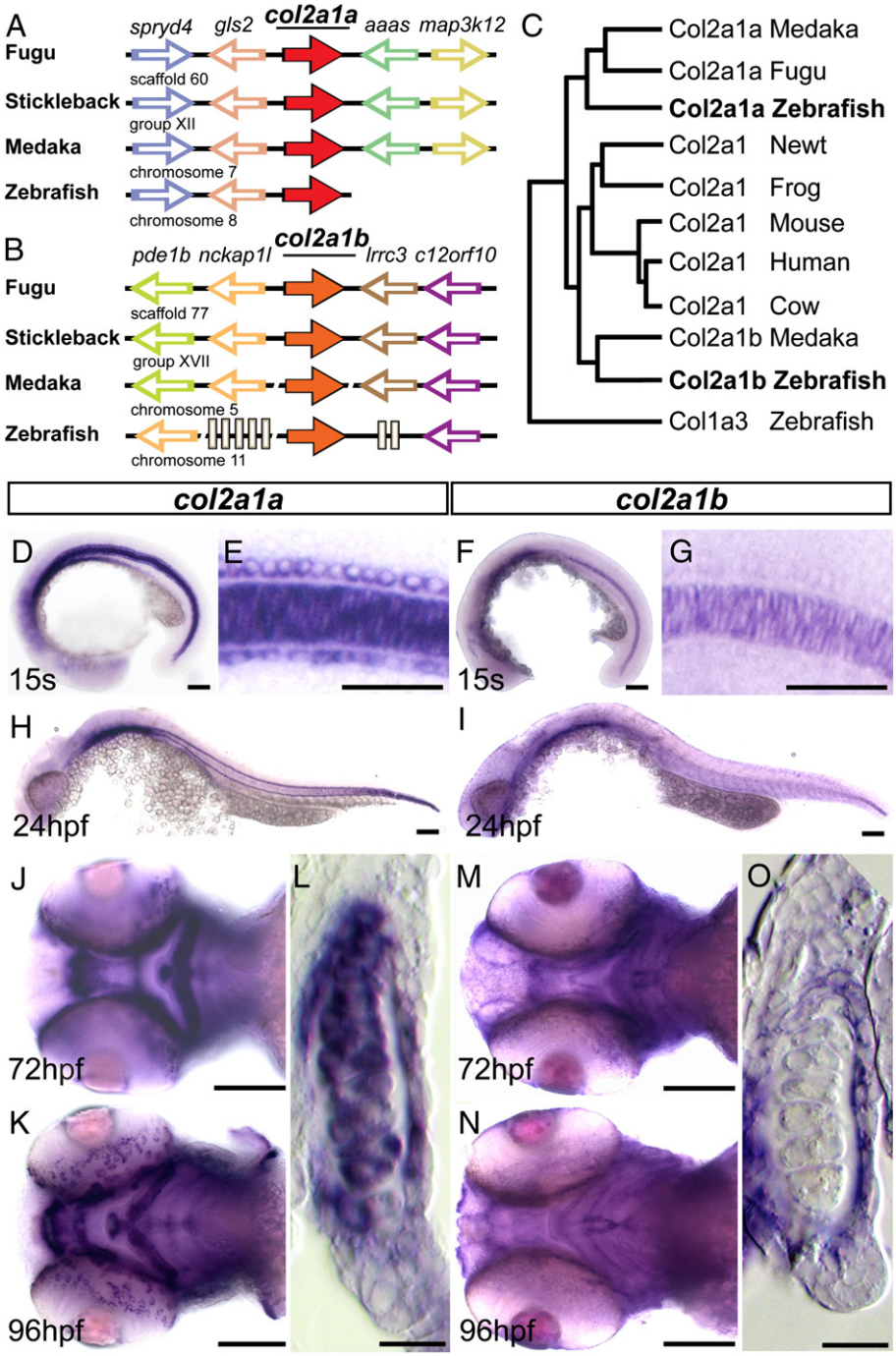

Fig. 1. Conservation and expression of zebrafish *col2a1* homologues. A–B. Schematic of conserved genomic synteny around the *col2a1a* (A) and *col2a1b* (B) genes in fugu, stickleback, medaka, and zebrafish with gene orientation marked by the direction of the arrows. Location of the genomic region is marked below. The angled slices through line denote gaps in the published sequence and grey boxes demark genes not conserved between teleosts. C. Phylogenic tree of the protein sequence between vertebrate *col2a1* homologues. D–O. Developmental expression patterns of *col2a1a* (D, E, H, J–L) and *col2a1b* (F, G, I, M–O) genes. D, F. Lateral view of a 15 somite stage embryo. E. Magnification of trunk region of the embryo shown on panel (D) with expression in the floor plate, notochord, and hypochord. G. Magnification of trunk of the embryo (F) showing only notochord expression. H, I. Lateral view of 24 hpf embryo. J, M. Ventral view of 72 hpf head. K, N Ventral view of 96 hpf head. L, O. Transverse section through ceratohyal cartilage and surrounding tissue of a 96 hpf embryo. Scale bars = 50 μm except for E, G, L and O = 25 μm.

much less noticeable in the *col2a1a* expression pattern, while strong expression of *col2a1a* in the endoderm was not observed in *col2a1b*. At the same time, *col2a1a* is beginning to be upregulated in the otic vesicle, and condensing chondrocytes of the pharyngeal arches and pectoral fins (Supplemental Figs. 1C,E). Both *col2a1* genes are expressed in the epidermis around the eye by 48 hpf.

Interestingly, *col2a1a* and *col2a1b* expression partially overlaps in the developing pharyngeal arches from 3 dpf onward (Figs. 1J–O). Beginning at 3 dpf we observed *col2a1a* expression within the stacking chondrocytes and the perichondrium (Figs. 1J–L), whereas *col2a1b* is expressed in the perichondrium only (Figs. 1M–O). By this time, expression of *col2a1b* has become very strong in the olfactory pits, which is not seen with the *col2a1a* probe (Figs. 1J,K,M,N). Based on the observed expression patterns for the two *col2a1* homologues, we concluded that *col2a1a* would be a better candidate for analysis for a regulatory element that drives expression in cartilaginous tissue.

Identification of a highly conserved regulatory element of col2a1a

While much work has been done to characterize the *col2a1* gene and its regulatory elements in mammals (Cameron et al., 2009; McAlinden et al., 2008; Ng et al., 1997; Seghatoleslami et al., 1995; Zhou et al., 1995), the enhancer region critical for cartilage and notochord expression of the zebrafish homologue has yet to be identified. A previously identified mouse enhancer region in the first intron and critical for mammalian expression (Zhou et al., 1995) is nonfunctional in zebrafish (Dr. Barbara Sisson, personal communication). Guided by strong expression within the craniofacial cartilage (Figs. 1J–L), we focused our search for putative cartilage regulatory elements around the *col2a1a* gene. To identify the transcriptional start site of *col2a1a*, we searched the available cDNA sequences in the NCBI expressed sequence tags (EST) database. We identified a properly spaced vertebrate TATA box, Downstream Promoter Element (DPE), and a likely transcriptional start site through our analysis of the genomic sequence around the region corresponding to the beginning of the longest 9 transcripts (Supplemental Fig. 2) (Smale and Kadonaga, 2003). All positions of regulatory elements are referenced from this putative +1 base (Fig. 2A, Supplemental Fig. 2).

To identify the regulatory element(s) that drives specific expression of *col2a1a* in cartilaginous tissues in the developing zebrafish, a comparative genetics approach was taken. The region analyzed included 8.5 kb upstream and 3.5 kb downstream of the transcriptional start site, including exons 1 and 2. Fugu, medaka, and stickleback genomic sequences corresponding to this zebrafish region were analyzed using the mVISTA program (Dubchak, 2007). This comparison identified four highly conserved genomic regions among all four fish (Fig. 2A). These regions are referred to as R1 (−7464 to −7259), R2 (−1720 to −1411), R3 (−389 to +1), and R4 (+2240 to +2445).

Despite similar expression of *col2a1b* in the notochord, a conserved sequence upstream of the open reading frame was not found. Inspection of the zebrafish genomic database revealed multiple gaps

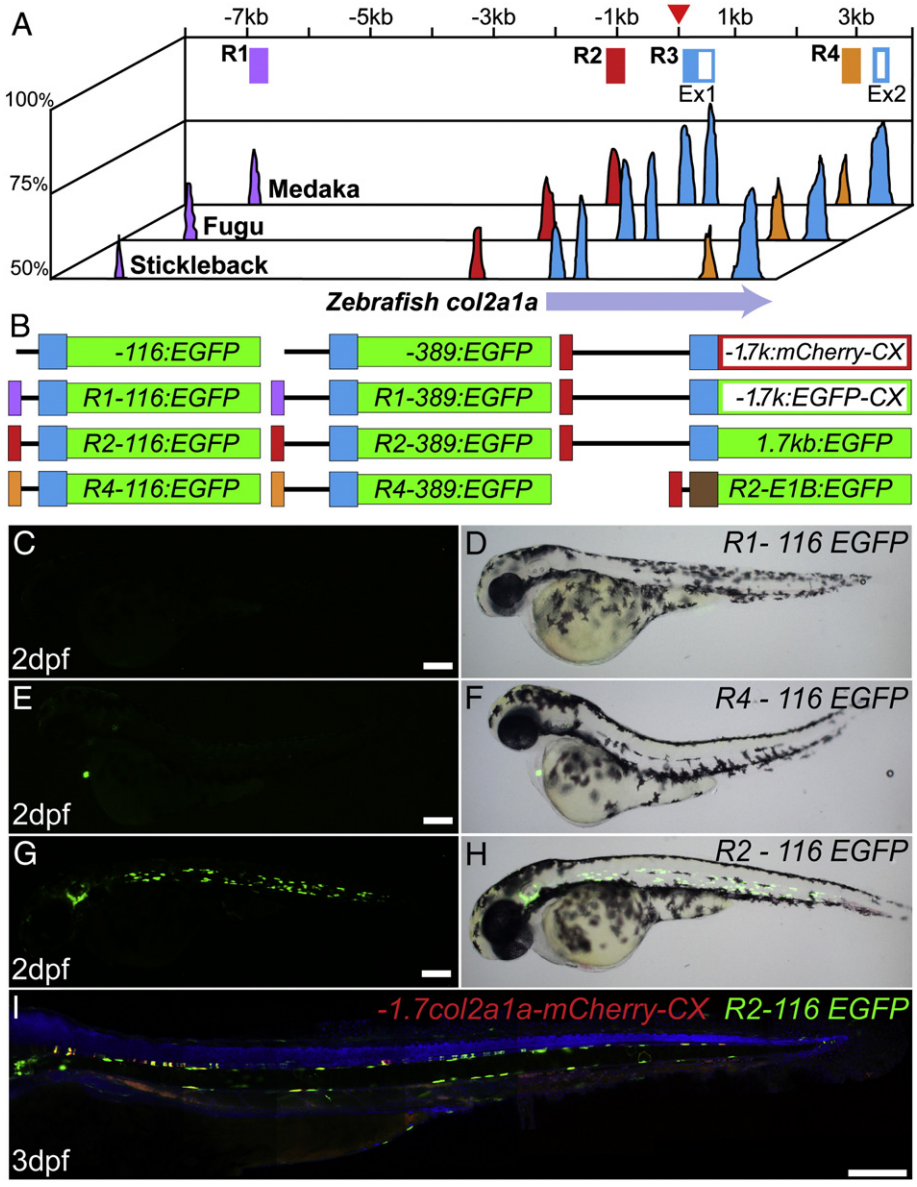

Fig. 2. Identification and characterization of evolutionally conserved elements of the *col2a1a* gene in teleosts. A. Schematic of an mVISTA plot comparing the 12 kb sequence around the transcriptional start site (red arrowhead) of the zebrafish *col2a1a* gene with corresponding regions of medaka, fugu, or stickleback. The X-axis represents genomic distance in kb away from the presumptive +1 transcriptional start site (red arrow head), the Y-axis represents percent homology over a 10 base pair window. Conserved domains used for regulatory analysis are schematized and color coded above the graph. Open boxes represent the coding sequence. B. Reporter constructs created during this study, with the color scheme of the regulatory elements as on panel A. C, E, G, Fluorescent and D, F, H, Nomarski image of embryos injected with plasmid DNA C-D *R1-116EGFP*, E-F *R4-116EGFP*, and G-H *R2-116EGFP*. I. Representative 3 dpf embryo injected with both *R2-116bp:EGFP* and −*1.7col2a1a:mCherry-caax* counterstained with DAPI. Scale bars = 200 μm.

in the sequence of this area, particularly where the predicted *col2a1b* conserved element would be located. Numerous attempts to amplify genomic fragments that would fill these gaps were unsuccessful (data not shown). The poor quality of the genome assembly in this area is likely due to the *col2a1b* gene's location at the telomeric region of chromosome 11 (Woods et al., 2005).

The newly identified R2 element is able to drive expression in the majority of the col2a1a domains

A recent report shows that a *Xenopus* conserved sequence, not present in mammals, just upstream of the transcriptional start site may be sufficient to drive expression in cartilage (Kerney et al., 2010). This *Xenopus* region, while not conserved between zebrafish and *Xenopus*, would map within the teleost conserved R3 domain as predicted by distance from the transcriptional start site. We generated two potential minimal promoters plasmids (−389:EGFP and −116:EGFP) which were injected at the one cell stage and then observed at 1 dpf for EGFP expression to determine if these fragments are sufficient to drive expression in zebrafish (Fig. 2B). Only faint ubiquitous EGFP expression was observed from the −389:EGFP promoter and no expression from the −116:EGFP (data not shown), suggesting that fish have a different organization of regulatory elements compared to *Xenopus* controlling expression of the *col2a1* homologue.

To test if the R1, R2, and R4 elements could recapitulate endogenous *col2a1a* expression, we cloned each of the conserved regions individually upstream of the −389 or −116 fragments and used EGFP as a reporter (Fig. 2B). We obtained similar mosaic expression using either the −389 or the −116 as a putative minimal promoter (Fig. 2 and data not shown). Observations at 1 through 3 dpf (Figs. 2C–H), revealed that the R1 element was unable to drive expression above background (Figs. 2C–D), suggesting that at least alone, it does not play a critical role in *col2a1a* expression. The R4 element was able to produce very weak expression at 1 dpf in the heart, ear and notochord but by 3 dpf this expression was undetectable (Figs. 2E–F). It is possible that R4 may cooperate with another regulatory element that drives endogenous expression but is not sufficient to drive and maintain expression on its own. The fusion of the R2 element to either of the minimal promoters produced strong EGFP expression from 1 through 3 dpf (n = 188 embryos) in multiple tissues, including the notochord, floor plate, ear, and cartilage (Figs. 2G–H), domains that correspond to normal *col2a1a* expression (Figs. 1H,J).

To further test if R2 alone is the critical regulatory element for *col2a1a* expression in zebrafish cartilage and notochord, the R2 element was fused to a minimal promoter containing a carp TATA box and the adenovirus E1b promoter upstream of EGFP, *R2-E1b:EGFP* (Koster and Fraser, 2001; Scheer and Campos-Ortega, 1999). More than 70 embryos positive for the *R2-E1b:EGFP* reporter displayed the same expression pattern as the *R2-116:EGFP* (Figs. 3C–D, 4H, and 5A–D).

To identify if there were any other zebrafish specific regulatory elements that cooperate with R2 in driving *col2a1a* expression and lay between it and the transcriptional start site, we generated a plasmid that contained the full 1.7 kb sequence from R2 through the initiation site driving a membrane localized red fluorescent marker (mCherry). Fish positive for the *−1.7 kb:mCherry-CAAX* (n = 230) exhibited the same expression pattern seen with R2 alone with a minimal promoter driving EGFP (Fig. 2I). These results demonstrate that the R2 region, which is conserved in teleosts, is sufficient to recapitulate a large portion of the normal expression of *col2a1a* (Figs. 1H,J and 2G–I).

To further characterize the activity of the *col2a1a* regulatory element, multiple transient and stable transgenic lines Tg(*1.7c2a1a:mgfp*) and (*R2c2a1a:gfp*) (see Materials and methods section for details) were generated and analyzed for reporter protein expression from 5 somites through adulthood. Transgene activity was detected in the cranial (Fig. 3) and axial (Fig. 6) cartilages, notochord (Figs. 4 and 5), floor plate and hypochord (Fig. 4), and ear (Fig. 6).

Embryonic expression of the col2a1a regulatory elements in craniofacial cartilage

Expression of *col2a1a* is observed in the zebrafish pharyngeal arches before craniofacial cartilage elements can be morphologically distinguished (Schilling and Kimmel, 1997; Yan et al., 1995) and is maintained until chondrocytes become hypertrophic and are replaced with bone (Figs. 1J–L). We were interested whether the isolated regulatory elements would be active in cranial chondrocytes. After co-injection of *−1.7kbcol2a1a:mcherry-CAAX* and *R2-E1b:EGFP* transgenes, EGFP and mCherry were detected in the pharyngeal arches at approximately 2.5 dpf, at which time the neural crest cells are condensing and differentiating into chondrocytes (data not shown). By 3 dpf the expression of both transgenes is detected in the chondrocytes and perichondrial cells of the developing craniofacial cartilages (Figs. 3A–B), which correlates with the endogenous expression of *col2a1a* (Fig. 1J). An examination of the stable lines revealed an increase in EGFP fluorescence by 36 hpf in newly condensing ectomesenchymal cells of the Tg(*1.7c2a1a:mGFP*) fish lines. The ceratohyal and trabeculae are the first cartilage elements to express EGFP (Fig. 3C, data not shown). As expected, the expression of EGFP in the Tg(*R2c2a1a:GFP*) was very similar to the Tg(*1.7c2a1a:mGFP*) line, but expression came on later around 48 hpf in the trabeculae (Fig. 3D).

Larval and adult expression of the col2a1a regulatory elements in craniofacial cartilage

At the early larval stage, Tg(*1.7c2a1a:mGFP*) and Tg(*R2c2a1a:GFP*) lines express EGFP in all pharyngeal and neurocranial cartilage elements (Fig. 3E). Strong expression of both reporter lines is maintained through adulthood in the head skeleton especially in the persistent growth plates and joints (Fig. 3F). In addition, we observed expression in the sutures of the adult skull (Fig. 3G).

Endochondrial bone formation in the zebrafish cranium begins at the larval stage, ~3.4 mm standard length (SL) (Cubbage and Mabee, 1996; Parichy et al., 2009) with the ossification of ceratohyal, hyomandibular, and Meckel's cartilages. There are other centers of ossification where bones are formed by intramembranous ossification, such as the operculum (Schilling, 2002). To compare the expression of the reporter in the context of these ossifications, transgenic fish were vitally stained with Alizarin Red (Kimmel et al., 2010) and observed every 7 days during the larval period (Figs. 3H–M). At 7 dpf, when larva reach 4.2 mm SL (here and throughout the text our SL refers to actual measurements of the specimen, see Materials and methods for full definition), one of the first cranial cartilages to ossify is the hyomandibula which is well positioned for live imaging. A reduction of EGFP expression was observed in the hyomandibular cartilage around 7 dpf (Fig. 3E). By 4.7 mm SL reporter activity is high in many cartilage elements of the skull, as rings of ossifying perichondrium form around the cartilage elements (Figs. 3H,K). We did not observe a significant decrease of reporter expression in the regions surrounded by newly formed periosteum, such as the ossification around ceratohyal cartilage at 4.7 mm SL (Fig. 5H). However, as endochondral ossification progresses, reduction in the cartilage expression is clearly visible (Figs. 3I,J). By 5.6 mm SL partial loss of reporter activity is observed in the palatoquadrate, symplectic, and the ceratohyal consistent with the progress of ossification (Figs. 3I,L). This loss of EGFP followed by the increase in Alizarin Red staining continues through the end of the larval period 29 dpf/7.8 mm SL (Figs. 3J,M).

Observing the development of the hyomandibular provides a good example of the progress of ossification and replacement of the cartilage mold by the bony matrix. At ~4.7 mm SL a sheath of bone forms on the surface just anterior and ventral to the facial nerve foramen (FF) (Fig. 3K). At ~5.6 mm SL within the sheath of Alizarin Red staining there is the loss of EGPF positive cells (Fig. 3L). By 7.8 mm SL a large part of the hyomandibular anterior and ventral to the foramen is

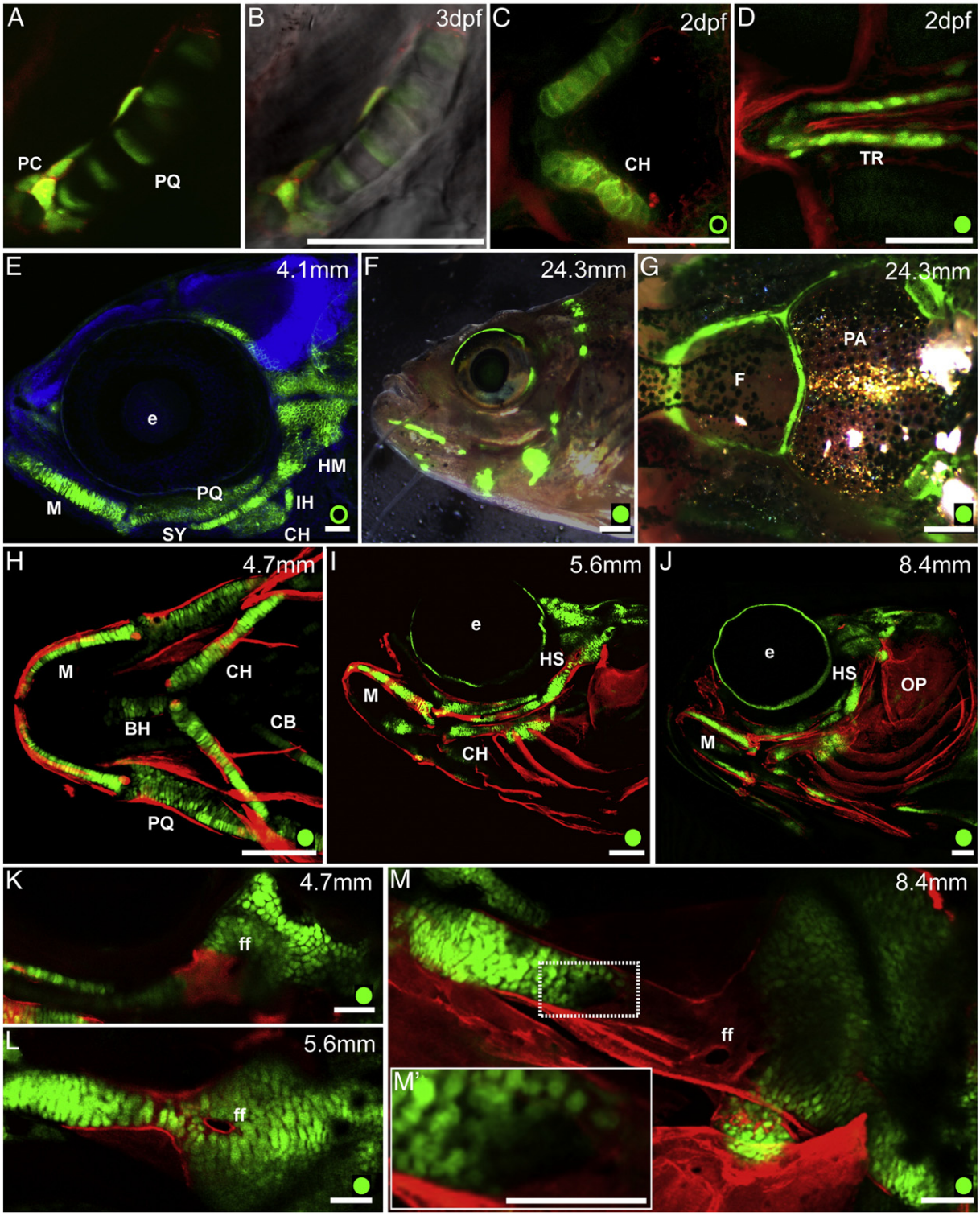

Fig. 3. Regulatory element R2 of the *col2a1a* gene drives expression in the craniofacial cartilages. A. Fluorescent and B. merged with Nomarski images of the palatoquadrate and surrounding perichondrium of an embryo injected with DNA for both *R2-E1b:EGFP* and *−1.7col2a1a:mCherry-caax*. C–D. Ventral view of 2 dpf embryos counterstained with wheat germ agglutinin conjugated to Alexa Fluor 647. A. Tg(*1.7c2a1a:mGFP*) is expressed in the ceratohyal. B. Tg(*R2c2a1a:GFP*) expression in the trabeculae. E. Lateral view of DAPI stained 4.1 mm SL Tg(*1.7c2a1a:mGFP*) embryo. F. Lateral view and G. dorsal view of head of adult Tg(*R2c2a1a:GFP*). H–J. Developmental time series of live larval stage Tg(*R2c2a1a:GFP*) fish stained with Alizarin red. H. Ventral view, I–J. Semi-lateral view. K–M. Lateral view of hyomandibular cartilages of H–J showing the process of ossification initiated ventral to facial nerve foramen. M′. Magnification of chondrocytes positive for EGFP as they begin the process of hypotrophy. Cartilages: BH, basihyal; CB, ceratobranchials; CH, ceratohyal; HM, hyomandibula; IH, interhyal joint; M, Meckel's, PQ, palatoquadrate; SY, symplectic; TR, trabeculae. Bones: F, frontal; OP, opercula; PA, parietal. Other: e, eye; ff, facial nerve foramen; pc, perichondrium; Scale bars: A–E, K–M = 50 μm, F = 500 μm, G = 400 μm, H–J = 150 μm. Here and throughout the paper a green circle marks Tg(*1.7c2a1a:mGFP*) and a green disk indicates the Tg(*R2c2a1a:GFP*).

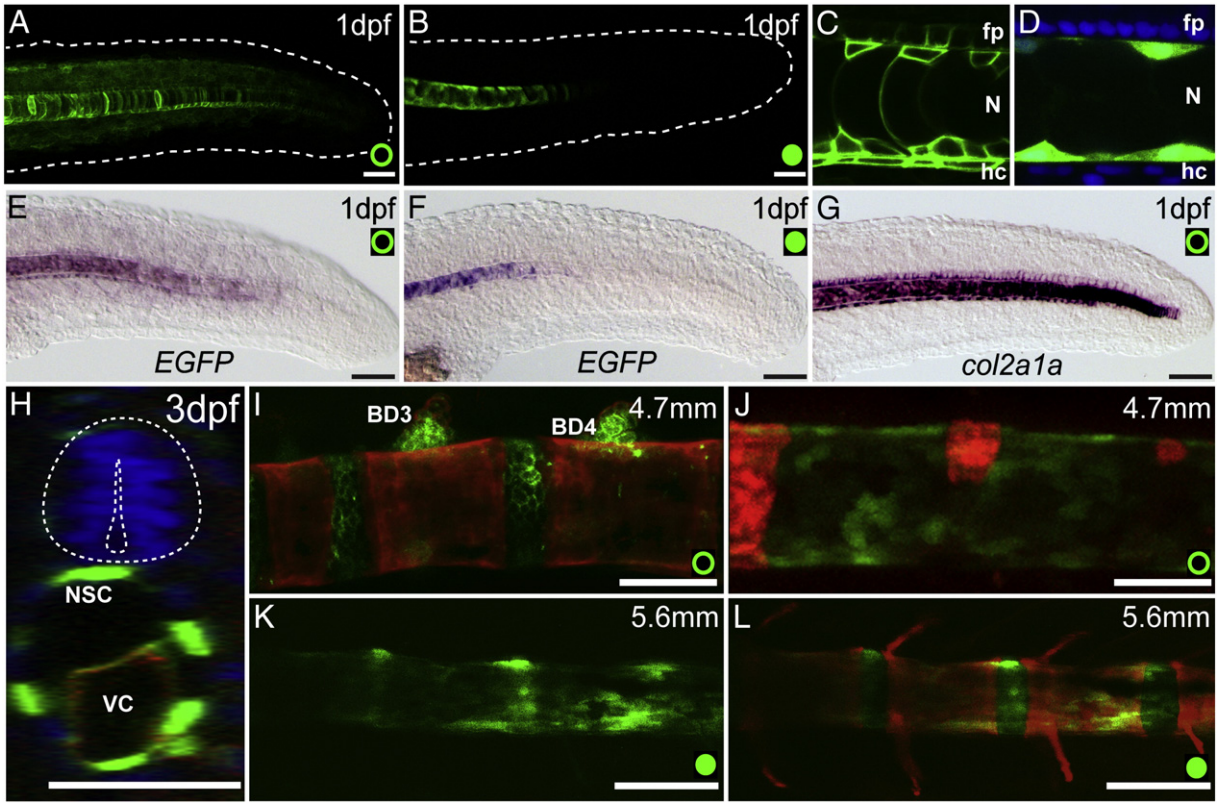

Fig. 4. Both transgenic lines drive expression in the developing notochord and other midline structures. A–B. Projection of the confocal image stacks of the posterior tail region of 1 dpf, lateral view. Outline of embryo is marked by white doted line. A. Tg(*1.7c2a1a:mGFP*) and B. Tg(*R2c2a1a:GFP*) embryos. C. Lateral view of mid-trunk of Tg(*1.7c2a1a:mGFP*) embryo showing EGFP expression (green) in the floor plate, hypochord, and notochordal sheath and vacuolated cells. D. Lateral view of mid-trunk of Tg(*R2c2a1a:GFP*) embryo showing EGFP expression (green) only in notochordal sheath cells. DAPI stained nuclei (blue) indicate position of the floor plate and hypochord. E–G. Lateral view of *in situ* hybridizations for *EGFP* (E–F) or *col2a1a* (G) expression at 1 dpf in (E, G) Tg(*1.7c2a1a:mGFP*) and (F) Tg(*R2c2a1a:GFP*). H. Orthogonal cross section of the confocal image Z-stack of 3 dpf embryo injected with *R2-116bp:EGFP* (green) and — *1.7col2a1a:mCherry-caax* (red) and counterstained with DAPI. Neural tube is outlined with white doted line. I–J. Notochord ossification of approximately a 14 dpf embryo. Anterior most (I) and posterior most (J) notochord ossification centra stained with Alizarin red. K–L. Approximately 21 dpf Tg (*R2c2a1a:GFP*) demonstrates transgenic activity is strongly reduced where centra are formed, but maintained in the region that will give rise to the intervertebral discs. Scale bar = 50 μm.

fully ossified and is no longer EGFP positive (Fig. 3M). Furthermore, stacked chondrocytes in the most ventral part of hyomandibular cartilage still express EGFP but as they change shape and undergo hypotrophy, EGFP expression fades in advance of positively stained Alizarin Red bone matrix that will replace the cartilage (Fig. 3M′). This process is reminiscent of the mammalian long bone growth plate (de Crombrugghe et al., 2000; Villemure and Stokes, 2009). This shows that our transgenes are useful markers of bone maturation not only through the presence but also the absence of GFP.

The zebrafish col2a1a regulatory element drives expression in the developing notochord and is maintained in the intervertebral disks

During early segmentation, 5 to 7 somites, the first tissue to show reporter activity downstream of both the 1.7 kb and the R2 elements is the developing notochord and this expression persists through adulthood (Fig. 4, data not shown). While both constructed regulatory elements have very similar expression, there are some differences between them in the forming midline tissues (Figs. 4A–F). Both lines show weak or absent EGFP florescence in the posterior tip of the notochord at 24 hpf. However, the EGFP fluorescence becomes visible earlier in the *Tg*(*1.7c2a1a:mGFP*) compared to the *Tg*(*R2c2a1a:GFP*) fish line (Figs. 4A,B). However, once established, expression in the notochord from both constructs is robust (Figs. 4I–L and 6I–L). The *Tg* (*1.7c2a1a:mGFP*) fish lines also show strong reporter expression along the floor plate and hypochord and are maintained through 36 hpf (Figs. 4A,C), whereas the *Tg*(*R2c2a1a:GFP*) stable lines do not have any obvious hypochord expression and only have a few GFP positive cells in the hindbrain floor plate (Figs. 4B,D; data not shown).

To determine if the lack of observed EGFP fluorescence was due to a lack of expression or to a delay required for GFP folding and accumulation of enough mature protein to be detected, we performed *in situ* hybridization against *EGFP* reporter transcript and compared it to the observed EGFP activity (Figs. 4A–F). The expression pattern of *EGFP* was similar to that observed by fluorescence, suggesting that the 1.7 kb fragment drives expression in the less differentiated notochord cells in addition to the floor plate and hypochord, where as the R2 element only drives expression in more mature notochord cells. Interestingly, in the *Tg*(*R2c2a1a:GFP*) fish a weak *EGFP* expression is seen by *in situ* hybridization in individual cells of the hypochord that was not observed by fluorescent microscopy (Fig. 4F). When compared with the endogenous *col2a1a* transcript, the reporter activity in both lines seems to be strong around the region of cells transitioning from thin stacked to large vacuolated cells where *col2a1a* expression usually begins to be down regulated (Figs. 4E–G).

The notochord arises from the cells of the axial mesoderm that intercalate to form a stack and then go through a process of vacuolation where the cells begin to swell and increase their size and shape from a pancake shape to a smooth large pebble (Halpern et al., 1993; Kimmel et al., 1995). Kimmel et al. (1995) described an additional type of cells that wrap the notochord as a "thin epithelial notochord sheath". In other fish this layer of cells has been referred to as the notochord sheath cells (NSC) (Grotmol et al., 2003). As the NSCs encase the notochord they express Col2a1 to build the extracellular matrix around the notochord (Grotmol et al., 2003, 2006; Kimmel et al.,

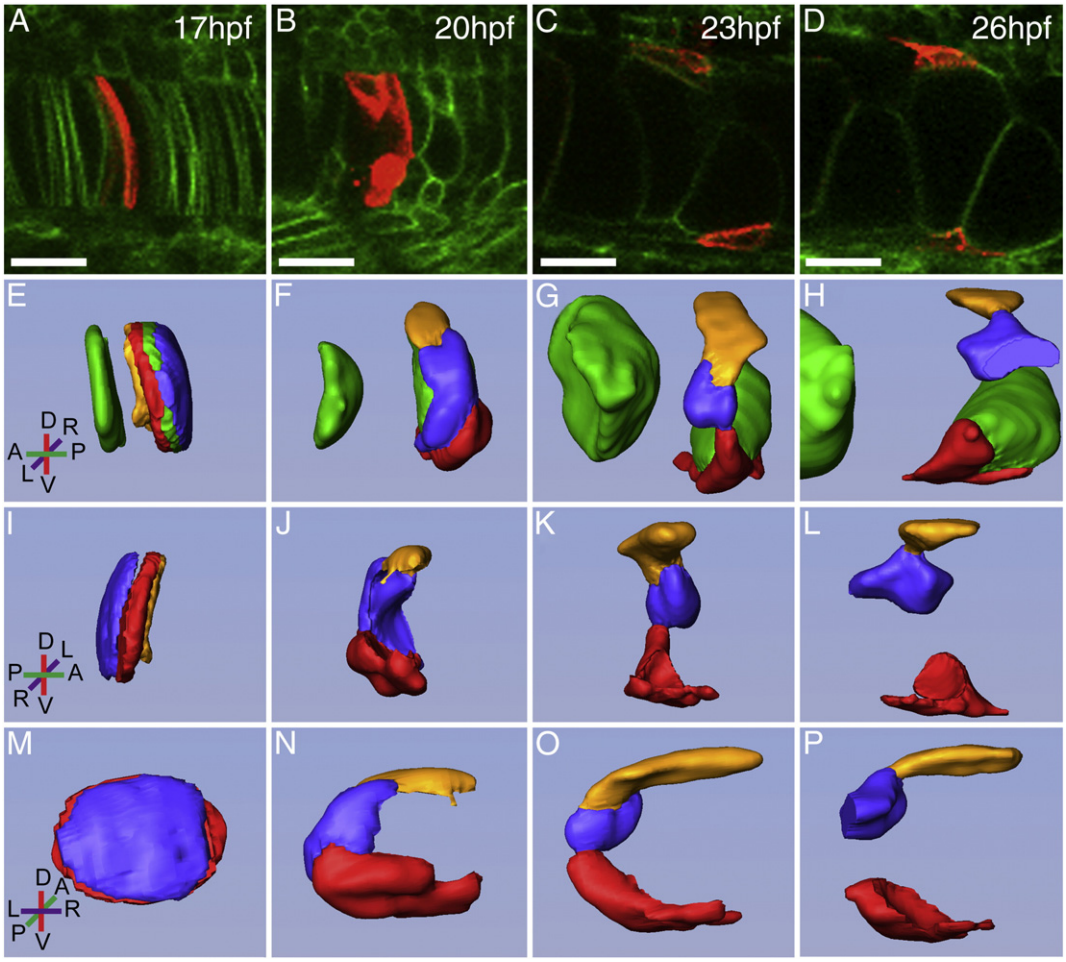

Fig. 5. Formation of the epithelial notochord sheath cells. (A–D) Confocal images of *Tg(β-actin:HRAS-EGFP)*^{vu119} fish injected with *−1.7kbcol2a1a:mCherry-CAAX* plasmid to track the snapping, retraction, and spreading process of NSCs over the course of 9 h. (E–P) 3D rendering of labeled cells from confocal images. (E–H) Lateral right and I–L. left lateral view with green vacuolated cells removed. (M–P) posterior view along notochord axis. Coordinates indicate anterior/posterior (A/P), dorsal/ventral (D/V), and left/right (L/R) axes. Scale bar = 20 μm.

1995). In both of our transgenic lines a thin single layer of cells that surrounds the notochord expresses the reporter (Figs. 4A–D,H). We predict the cells in this layer to be the NSCs that have been previously reported (Kimmel et al., 1995; Koster and Fraser, 2001; Yamamoto et al., 2010). We took advantage of our reporter constructs to track the formation of the NSC layer as described in the following section.

The ossification of the notochord occurs in regions called centra that form in an anterior to posterior order (Bird and Mabee, 2003). Centra are separated by regions of non-ossifying notochord cells, which give rise to the intervertebral disks (IVD). By staining transgenics *in vivo* with Alizarin Red, the process of notochord ossification can be easily observed by confocal imaging (Figs. 4I–L). By the mid-larval stage of 4.7 mm SL distinct rings of mineralized tissue form around the anterior notochord in a ventrad fashion (Figs. 4I,J). Both stable transgenic lines gradually lose EGFP expression in the NSC underling ossifying centra but maintain it in the prospective IVD (Fig. 4I). Furthermore, both stable transgenics show expression of GFP in basidorsal 3 and 4, which give rise to neural arches 3 and 4 of the otophysans conserved Weberian apparatus that connects the ear to the swim bladder (Fig. 4I) (Bird and Mabee, 2003; Grande and Young, 2004).

When the larva has reached approximately 5.3 mm SL the ossified centra begin to form the stereotypic hourglass shape and the EGFP transgenic activity in those regions is almost gone. In contrast, the expression of EGFP in the regions that will give rise to the IVDs is still strong and remains so throughout adulthood (Figs. 4K,L, and data not shown).

The col2a1a regulatory elements allow detailed mapping of the process of notochord cell vacuolation and notochord sheath formation

Recent work has demonstrated that the decision of a notochord cell to be a vacuolated cell (VC) or to become a NSC is dependent on Notch signaling (Yamamoto et al., 2010). However, tracking the morphogenesis of these cells has been challenging. The strong expression of our fluorescent *col2a1a* reporters in NSCs, in contrast to weaker expression in the VCs, allowed us to investigate the details of this process (Fig. 5).

By injecting the *−1.7kbcol2a1a:mcherry-CAAX* plasmid into the *Tg(βactin:HRAS-EGFP)*^{vu119} fish line, in which all cells of the fish express a membrane localized EGFP, individual cells of the notochord were mosaically marked red. Using time-lapse confocal microscopy we were able to observe the maturation process of the notochord from 17 to 26 hpf in 12 embryos in the tail just posterior to the end of the yolk extension (Figs. 5A–D, Supplemental Movie 1). In this interval a wave of cellular vacuolation migrates posteriorly. At the crest of the wave front, some cells enlarge and will become the smooth pebble shape VC cells in the center of the notochord, while a larger number of flat notochord cells withdraw from the stack towards the edge of the notochord and become the NSC layer (Figs. 5A–H). These initially symmetrical, discoid NSCs appear to lose contact with the periphery of the notochord and "snap" at one side and subsequently "retract" to the opposite side of the notochord, which they remained attached to. As the NSCs retract they begin to spread across the periphery of the notochord to cover the enlarging VCs. This "snapping, retraction, and

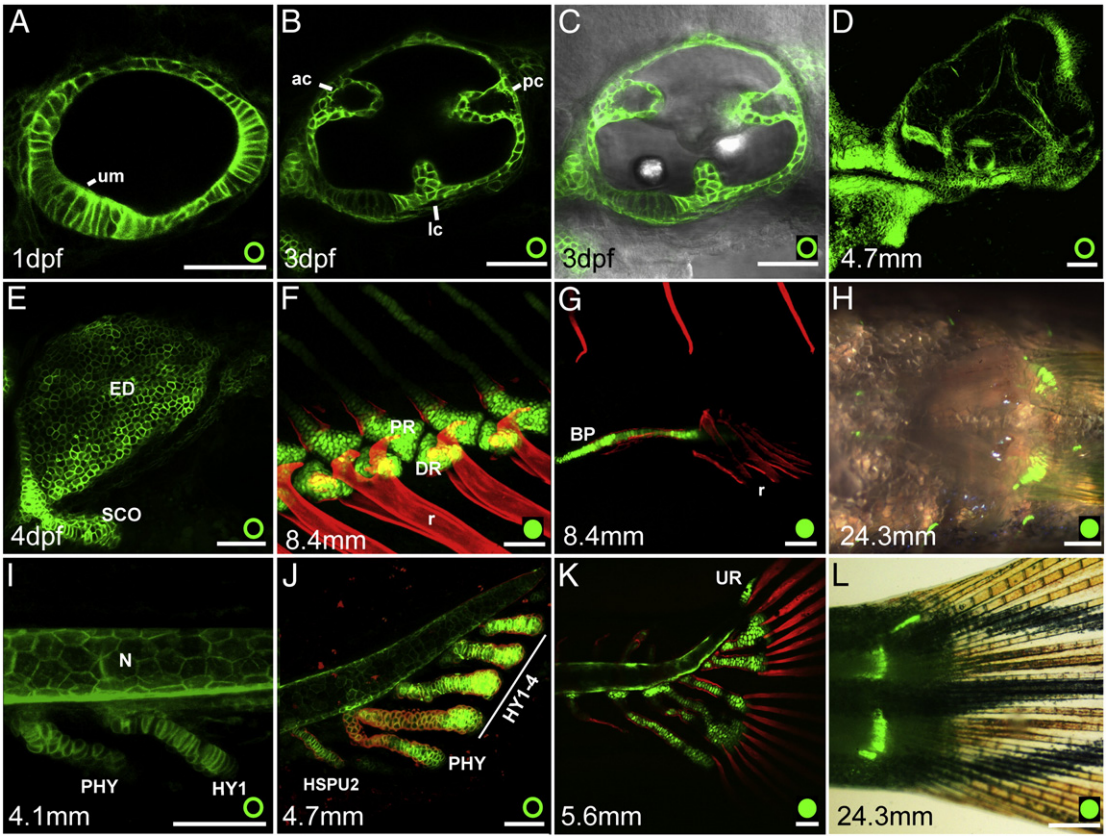

Fig. 6. Expression of the reporter proteins in the developing ear and fin structures. A–D. Developmental time series of ear development from 1 dpf to 14 dpf (~4.7 mm SL). E. 4 dpf zebrafish pectoral fin. F. Anal and G–H. pelvic fins. I–L. Formation of the skeleton of the caudal fin support from 7 dpf till adulthood. ac, anterior canal; BP, basipterygium; DR, distal radial; ED, endochondrial disc; HY, hypurals; HSPU, hemal spines. lc, lateral canal; N, notochord; pc, posterior canal; PHY, parhypural; PR, proximal radial; R, ray; SCO, scapulocoracoid; UR, urostyle, um; utricular macula; Scale Bars = 50 μm except for H, L = 2 mm.

spreading" process occurs in less than 2 h and is well coordinated between cells so that as the VC increase their volume and the diameter of the notochord, NSC precursors start to reposition to form a single layer of flat cells surrounding the notochord (Figs. 5I–P, Supplemental Movie 1).

To identify the percentage of the stacked notochord cells that contribute to the formation of NSCs, developing notochord cells with labeled membrane GFP and DAPI were divided into three zones, Stacking, Retraction and Vacuolation (Supplemental Fig. 3). Because the floor plate is made up of stereotypical shaped cells that run along the entire notochord, it is an excellent marker to use as a unit of distance for each zone. By comparing the number and location of nuclei in each zone in four embryos we found that 10 floor plate cells in each zone correspond to approximately 33 ± 10 notochord cells. In the Stacked zone, 100% of the nuclei were in the middle of the notochordal space. In the Retraction zone, we observed that on average only 43% ± 7 of the nuclei were in the middle of the space, whereas the rest were located at the periphery of the notochordal space. Interestingly, in the Vacuolation zone only 21% ± 6 of the nuclei were in the middle of the notochordal space and the majority (79% ± 6) of the cells had migrated to form the notochordal sheath (Supplemental Fig. 3). This analysis demonstrates that the bulk of the cells stacked in the newly formed zebrafish notochord are destined to differentiate into NSCs.

The col2a1a regulatory elements drive expression in the developing ear

Another region with strong expression of the *col2a1a* is the developing ear. The zebrafish ear arises from ectodermal cells that are induced by signals from the adjacent mesendoderm and hindbrain to form the otic placodes which becomes the otic vesicles (Whitfield et al., 2002). The epithelial cells of the otic vesicle produce the neurons and semicircular canals of the adult ear (Haddon and Lewis, 1996; Whitfield et al., 2002). Expression of *col2a1a* in the developing ear begins as early as 18 somites in the epithelium of the otic vesicle (Yan et al., 1995). In our stable transgenic lines the first ear expression is observed at the end of segmentation and the beginning of the pharyngula stage, ~1 dpf, in the epithelial lining of the otic vesicle including the cells of the maculae which produce the sensory hair cells (Fig. 6A). During the hatching to larval stages, 2 to 4 dpf, the otic vesicle matures to form the semicircular canal system of the ear and increased thickening of the maculae, all of which show transgene expression but with weaker expression in the sensory patch (Figs. 6B–C). By the end of the second week of development (~4.7 mm SL) the ear has undergone further morphogenesis, however, the cells making up the semicircular canals are all still positive for reporter activity (Fig. 6D) and can still be observed through to adulthood (data not shown).

The cartilaginous skeletal elements of the fins maintain col2a1a reporter activity throughout life

The zebrafish has two sets of paired fins, pectoral and pelvic, and three unpaired fins, dorsal, anal, and caudal. The adult pectoral fin skeleton is made up of both dermal and endochondral bones (Cubbage and Mabee, 1996; Schilling, 2002). Endogenous *col2a1a* expression is observed in the developing scapulocoracoid cartilage and the endochondral disc of the pectoral fin by 48 hpf (Yan et al., 1995). Consistent with endogenous *col2a1a* expression, we also observed reporter activity in these cartilage structures (Fig. 6E). By the end of the larval stage (~8.4 mm SL) in addition to the pectoral fin, reporter expression is observed in the radials of the anal fin (Fig. 6F) and the

basipterygium of the pelvic fin (Fig. 6G). Interestingly, unlike the pectoral fin, which has an embryonic appendage that precedes it, the pelvic fin directly forms into the adult structure (Schilling, 2002). In adult transgenic animals both basipterygium and radials of pelvic fin strongly express EGFP (Fig. 6H).

The zebrafish caudal fin and its support structures form on the ventral side of the notochord as a mesenchymal condensation, but due to the dorsal flexion of the notochord when larva reach 4.5 mm SL it is positioned along the anterior–posterior body axis (Bird and Mabee, 2003; Parichy et al., 2009). The support skeleton of the caudal fin is composed of hemal and neural arches and spines. In the developing caudal fin, transgene expression is first detected in the parhypural and the first hypural around 4.1 mm SL (Fig. 6I). The parhypural and hypurals are derived from the ventral hemal arches and spines of the dorsally bent notochord and at first are separate chondrocyte condensations at ~3.7 mm SL (Bird and Mabee, 2003). By 4.7 mm SL the transgenic fish express EGFP in the spines of the preural vertebrae, the parhypural and 4 of the 6 hypurals (Fig. 6J). The presence of Alizarin Red within the parhypural and the first hypural indicates ossification within these structures, and the first signs of ossification can also be seen within the second hemal spines of the preural vertebrae and hypurals 2–4 (Fig. 6J). By 5.6 mm SL, all the second hemal spines of the preural vertebrae, the parhypural, the 5 hypurals, and the urostyle are formed (Bird and Mabee, 2003; Parichy et al., 2009) and express EGFP (Fig. 6K). In adult fish, the *col2a1a* regulatory element is still active in the most caudal tip of notochord, the urostyle, and in hypural growth plates (Fig. 6L). Similar to the craniofacial cartilages, ossification of the hypurals leads to the decreased expression of the reporter in the proximal part of the elements as compared to the less differentiated distal parts.

Loss of sox9a down regulates col2a1a regulatory element R2 activity in craniofacial cartilage, but not in the developing ear or notochord

In mammals, *sox9* regulates *Col2a1* and other genes critical for cartilage and bone formation (Akiyama et al., 2002). In zebrafish, the loss of *sox9a* down regulates *col2a1a* expression and causes the reduction and loss of cranial and pectoral fin cartilage elements, such as Meckel's cartilage and the scapulocoracoid of the fin (Yan et al., 2002; Yan et al., 2005). To test if the knockdown of *sox9a* had a similar effect on the activity of the R2 regulatory element we injected a splice-junction morpholino against *sox9a* mRNA (Yan et al., 2002) into zebrafish embryos at the 1–2 cell stage. Injected embryos were observed daily from 1 to 4 dpf for EGFP expression. At 1 dpf notochord expression was similar between injected and uninjected siblings (Figs. 7A,E). At 2 dpf, expression in the developing otic vesicle was also not significantly different (data not shown). In contrast, by 4 dpf reporter expression was noticeably reduced or absent in the cranial cartilages and the pectoral fins (Figs. 7C–D, G–H and data not shown), while expression in the ear and notochord was still similar (Figs. 7B,F and data not shown). This suggests that the R2 based transgenic line responds to the knockdown of Sox9a in the craniofacial cartilages in the same way as endogenous *col2a1a* gene.

Discussion

Evolution of the col2a1 genes

Unlike terrestrial vertebrates, zebrafish have two homologues of the *col2a1* gene; *col2a1a* and *col2a1b* (Fig. 1). Recent work has demonstrated that two *col2a1* genes were present before the split of the vertebrates into the Agnatha and Gnathostomata clades as both hagfish (Ota and Kuratani, 2010) and lamprey (Zhang et al., 2006a) have two *col2a1* genes with expression domains common with fish and mammals (Ota and Kuratani, 2010; Zhang et al., 2006a). In all tested fish both *col2a1* genes maintain the genomic synteny for each gene's homologue (Fig. 1B). Interestingly, the region of zebrafish chromosome 11 containing the *col2a1b* gene is syntenic with the region of human chromosome 12 encoding *COL2A1* (Woods et al., 2005) but to a region that is about 10 Mb away from *COL2A1*. Based on our comparison of the genomic regions surrounding the two *col2a1* genes, we propose that these genes are not paralogues arising from a whole genome duplication observed in teleosts, but are homologues of two genes present in the ancestral craniate with the loss of one gene in the evolution of tetrapods.

Genomic comparisons among teleosts can identify functional regulatory elements

While comparative genomics is a powerful tool for identifying functional evolutionarily conserved sequences among organisms, comparing very evolutionarily distant genomes, such as fish and mammals,

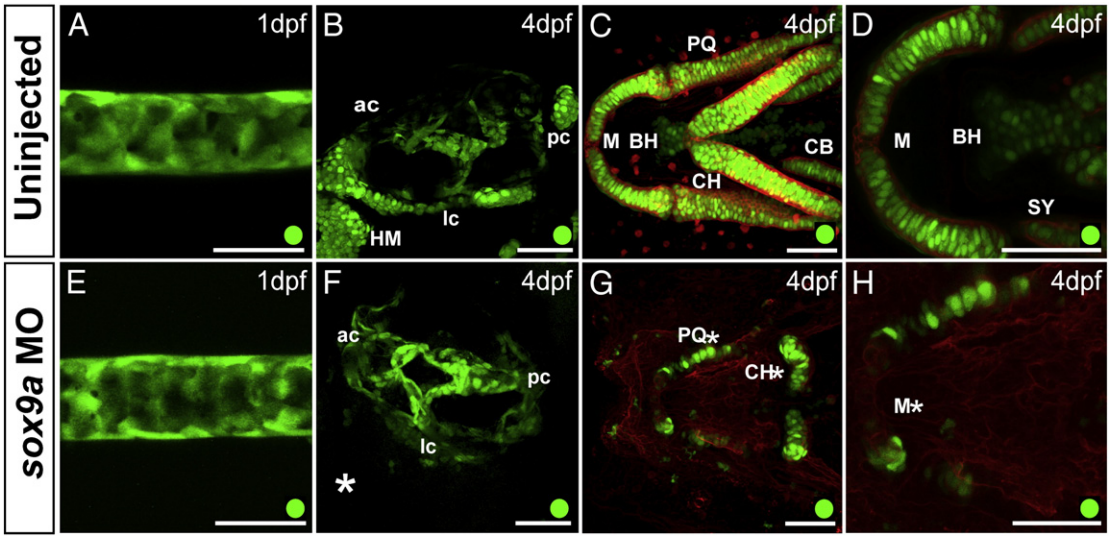

Fig. 7. Loss of Sox9a affects R2 activity in cartilage, but not in ear or notochord. A–D. Uninjected sibling and E–H. *sox9a* morphant of Tg(*R2c2a1a:GFP*). A, E. Lateral view of the notochord of 1 dpf embryo. B, F. Lateral view of 4 dpf embryo ear. C, G. Ventral view of craniofacial cartilage of 4 dpf embryo. D, H. Higher magnification of C,G. (respectively) focused on Meckel's Cartilage. ac, anterior canal; BH, basihyal; CB, ceratobranchials; CH, ceratohyal; HM, hyomandibular; lc, lateral canal; M, Meckel's cartilage; pc, posterior canal; PQ, palatoquadrate; SY, symplectic. Scale bars = 50 μm.

may not detect conserved regions of interest while the sequence in question may contain a real regulatory element (Kague et al., 2010; Punnamoottil et al., 2010). The probability of a deletion, mutation, or relocation of a critical regulatory elements increases with the evolutionary distance as when comparing genomes as far apart as teleosts and mammals. In this study we used the available teleost genomic sequence data around the *col2a* homologues and the relative evolutional range within these species, to identify conserved nucleotide regions that could be experimentally verified where a similar comparison to mammalian genomes is not beneficial (Fig. 2A and data not shown).

Functional differences between the −1.7 and R2 regulatory units

The R2 regulatory element is able to drive expression of reporter genes in cartilage (Fig. 3), notochord (Figs. 4 and 5), and ear (Fig. 6). We also created a longer reporter, a 1.7 kb promoter fragment (Fig. 2B) that spanned from R2 to the transcriptional initiation site, to determine if this fragment may enhance R2 expression by providing non-conserved zebrafish specific regulatory elements. Stable transgenic lines were generated for the R2 and 1.7 kb sequence. Both *Tg*(*1.7c2a1a:mEGFP*) and Tg(*R2c2a1a:GFP*) lines demonstrated similar reporter expression with a few exceptions. Unlike the *Tg*(*1.7c2a1a:mEGFP*) embryos, the R2 based stable transgenics only express reporter protein in the notochord and not the floor plate (Figs. 4A–D). Also the posterior extent of the reporter transcript is further in the 1.7 kb versus the R2 lines. This suggests that some elements needed for robust early expression in the nascent notochord are absent in the 1.7 kb fragment, and the floor plate and hypochord specific elements are further missing from the R2 element. In addition to the newly formed notochord, both transgenic lines lack expression in some domains as compared to the endogenous expression of *col2a1a*. For example, we did not detect endodermal expression on the first day of development or in the regenerating caudal fin (data not shown) (Johnson and Weston, 1995; Yan et al., 1995).

The Tg(*1.7c2a1a:mEGFP*) lines exhibit a low level of EGFP expression in the epidermis and in the head mesenchyme for the first 36 to 48 h of development, which is quickly lost by 3 dpf. This low level of basal expression was also seen in the transient fish lines made with the endogenous *col2a1a* minimal promoter (*−389:EGFP*). As the *−1.7kbcol2a1a:EGFP-CAAX* plasmid contains this −389 bp sequence, we suspect that this less restricted expression is due to its presence, further suggesting that it is the minimal promoter for *col2a1a* and unlike in *Xenopus* is not required for cartilage specific expression (Kerney et al., 2010).

Understanding notochord cell morphogenesis

The nascent zebrafish notochord is composed of stacked cells that by the middle of the second day of development form two cell types: vacuolated cells (VC) and notochord sheath cells (NSC). Using our regulatory element we were able to scatter-label stacked notochord cells and track in high detail their morphogenesis from a single stack of cells to form a structure composed of VCs surrounded by a single layer of NSCs (Fig. 5, Supplemental Movie 1). This analysis identified that the process of NSC retraction from the stack is relatively quick (~2 h) and most of the notochord cells form epithelial NSC. This is a great model for studying cellular behaviors underlying the disassembly of cellular stacks, a process possibly taking place during the formation of other cartilaginous elements.

As development progresses the notochord ossification results in the formation of mineralized rings that will later develop into vertebrae that are separated by cartilaginous discs (Fig. 3J). While details of this process are different in salmon, medaka and zebrafish, the mineralization of the notochord sheath is observed in all these species. While GFP expression is eventually lost in the regions that will give rise to vertebrae (Figs. 3K–L), GFP expression is maintained in the epithelial cells surrounding parts of the notochord that will give rise to the intervertebral discs. Thus our new transgenic lines, with the strong and long lasting activity of the R2 element, should be a good tool for the study of disc formation and maintenance and the loss of reporter activity will be beneficial in studying cartilage hypotrophy and endochondral bone formation.

The col2a1a regulatory unit as a tool to monitor cartilage formation and maturation

The goal of this work was to identify a regulatory element that would allow for targeted gene expression in cartilage. With the help of these new regulatory elements we are able to recapitulate much of the endogenous *col2a1a* expression. In comparison to available regulatory elements, the *col2a1a* fragments described here allow for targeted gene expression in cartilaginous tissues from embryonic to adult stages without driving expression in precursor cells, such as the cranial neural crest. We also demonstrated that the R2 element functions similarly to the endogenous *col2a1a* cartilage driver as R2 is down regulated by the loss of *sox9a*, a gene required for proper craniofacial cartilage formation.

While both of the *col2a1a* reporter lines are expressed well in the developing cartilage (Fig. 3), they also show the process of endochondral ossification by identifying the hypertrophic zone of an element (Figs. 3K–M′). As chondrocytes begin to hypertrophy, they begin to shut down cartilage specific genes, such as *col2a1a* (Sandberg and Vuorio, 1987). Therefore, we would expect the loss of EGFP from chondrocytes as they start the process of hypertrophy. However, we detected the presence of EGFP longer than this possibly due to the stability of the protein, which can persist for days after its gene expression is shut down. Future work will be to design a transgenic plasmid that allows for quicker degradation of reporter genes under the control of *col2a1a*.

Interestingly, one of the obtained alleles of the *Tg*(*1.7c2a1a:mEGFP*)^{nu17} produces a weaker mosaic expression of EGFP (data not shown). This mosaic expression is most likely due to random silencing of the transgene, as this pattern of expression has been maintained through at least two generations. This allele will be very useful for "scatter-labeling" for the study of individual cell migration during tissue morphogenesis. Such scatter-labeling of the chondrocytes has previously been achieved by injection of rhodamine-dextran into a group of cells at the mid- to late blastula stage, yielding a variable number of cells labeled in the cartilage element of interest (Kimmel et al., 1998). By utilizing this transgenic, or through DNA injection of our *col2a1a* regulatory plasmids, one would be able to specifically target scattered fluorescent expression in the cartilage, notochord, and ear.

The relatively small size of the R2 regulatory unit allows for it to be easily manipulated and used for targeted gene expression without having to deal with large genomic fragments or BACs that can be problematic to work with or limit the size of gene desired to be driven. All of the identified regulatory elements were generated with the Gateway system (Invitrogen) so they can be used with the versatile zebrafish Tol2 system allowing for quick generation of transgenic plasmids and fish (Kwan et al., 2007). Based on our observations, the early diffuse expression of the *−1.7 kb col2a1a* fragment in the head mesenchyme and early chondrocyte condensation and stacking would be a good driver of gene expression to allow for targeted gene expression at the onset of chondrocyte stacking with a low level of background, whereas the *R2 col2a1a* unit could be used for later expression during stacking in a more restricted manner.

Supplementary materials related to this article can be found online at doi:10.1016/j.ydbio.2011.06.020.

Acknowledgments

We would like to thank Dr. Jolanta Topczewska, Dr. Barbara Sisson, Dr. Elizabeth LeClair and Mr. G. Parker Flowers for critical review of

the manuscript and providing unpublished results and Mr. William Goossens for providing microscopy assistance. This work was funded by the National Institutes of Health's National Institute of Dental and Craniofacial Research (grants R01DE016678 to JT and F32DE019986 to RMD).

References

Akiyama, H., Chaboissier, M.C., Martin, J.F., Schedl, A., de Crombrugghe, B., 2002. The transcription factor Sox9 has essential roles in successive steps of the chondrocyte differentiation pathway and is required for expression of Sox5 and Sox6. Genes Dev. 16, 2813–2828.

Bird, N.C., Mabee, P.M., 2003. Developmental morphology of the axial skeleton of the zebrafish, *Danio rerio* (Ostariophysi: Cyprinidae). Dev. Dyn. 228, 337–357.

Boot-Handford, R.P., Tuckwell, D.S., 2003. Fibrillar collagen: the key to vertebrate evolution? A tale of molecular incest. Bioessays 25, 142–151.

Cameron, T.L., Belluoccio, D., Farlie, P.G., Brachvogel, B., Bateman, J.F., 2009. Global comparative transcriptome analysis of cartilage formation *in vivo*. BMC Dev. Biol. 9, 20.

Catchen, J.M., Conery, J.S., Postlethwait, J.H., 2009. Automated identification of conserved synteny after whole-genome duplication. Genome Res. 19, 1497–1505.

Cheah, K.S., Stoker, N.G., Griffin, J.R., Grosveld, F.G., Solomon, E., 1985. Identification and characterization of the human type II collagen gene (COL2A1). Proc. Natl. Acad. Sci. U. S. A. 82, 2555–2559.

Cheah, K.S., Lau, E.T., Au, P.K., Tam, P.P., 1991. Expression of the mouse alpha 1(II) collagen gene is not restricted to cartilage during development. Development 111, 945–953.

Corpet, F., 1988. Multiple sequence alignment with hierarchical clustering. Nucleic Acids Res. 16, 10881–10890.

Crump, J.G., Swartz, M.E., Eberhart, J.K., Kimmel, C.B., 2006. Moz-dependent Hox expression controls segment-specific fate maps of skeletal precursors in the face. Development 133, 2661–2669.

Cubbage, C.C., Mabee, P.M., 1996. Development of the cranium and paired fins in the zebrafish *Danio rerio* (Ostariophysi, Cyprinidae). J. Morphol. 229, 121–160.

de Crombrugghe, B., Lefebvre, V., Behringer, R.R., Bi, W., Murakami, S., Huang, W., 2000. Transcriptional mechanisms of chondrocyte differentiation. Matrix Biol. 19, 389–394.

Dubchak, I., 2007. Comparative analysis and visualization of genomic sequences using VISTA browser and associated computational tools. Methods Mol. Biol. 395, 3–16.

Dutton, J.R., Antonellis, A., Carney, T.J., Rodrigues, F.S., Pavan, W.J., Ward, A., Kelsh, R.N., 2008. An evolutionarily conserved intronic region controls the spatiotemporal expression of the transcription factor Sox10. BMC Dev. Biol. 8, 105.

Exposito, J.Y., Valcourt, U., Cluzel, C., Lethias, C., 2010. The fibrillar collagen family. Int. J. Mol. Sci. 11, 407–426.

Grande, T., Young, B., 2004. The ontogeny and homology of the Weberian apparatus in the zebrafish *Danio rerio* (Ostariophysi: Cypriniformes). Zool. J. Linn. Soc. 140, 241–254.

Grotmol, S., Kryvi, H., Nordvik, K., Totland, G.K., 2003. Notochord segmentation may lay down the pathway for the development of the vertebral bodies in the Atlantic salmon. Anat. Embryol. (Berl) 207, 263–272.

Grotmol, S., Kryvi, H., Keynes, R., Krossoy, C., Nordvik, K., Totland, G.K., 2006. Stepwise enforcement of the notochord and its intersection with the myoseptum: an evolutionary path leading to development of the vertebra? J. Anat. 209, 339–357.

Haddon, C., Lewis, J., 1996. Early ear development in the embryo of the zebrafish, *Danio rerio*. J. Comp. Neurol. 365, 113–128.

Halpern, M.E., Ho, R.K., Walker, C., Kimmel, C.B., 1993. Induction of muscle pioneers and floor plate is distinguished by the zebrafish no tail mutation. Cell 75, 99–111.

Halpern, M.E., Hatta, K., Amacher, S.L., Talbot, W.S., Yan, Y.L., Thisse, B., Thisse, C., Postlethwait, J.H., Kimmel, C.B., 1997. Genetic interactions in zebrafish midline development. Dev. Biol. 187, 154–170.

Han, Y., Lefebvre, V., 2008. L-Sox5 and Sox6 drive expression of the aggrecan gene in cartilage by securing binding of Sox9 to a far-upstream enhancer. Mol. Cell Biol. 28, 4999–5013.

Hattori, T., Coustry, F., Stephens, S., Eberspaecher, H., Takigawa, M., Yasuda, H., de Crombrugghe, B., 2008. Transcriptional regulation of chondrogenesis by coactivator Tip60 via chromatin association with Sox9 and Sox5. Nucleic Acids Res. 36, 3011–3024.

Hoornaert, K.P., Vereecke, I., Dewinter, C., Rosenberg, T., Beemer, F.A., Leroy, J.G., Bendix, L., Bjorck, E., Bonduelle, M., Boute, O., Cormier-Daire, V., De Die-Smulders, C., Dieux-Coeslier, A., Dollfus, H., Elting, M., Green, A., Guerci, V.I., Hennekam, R.C., Hilhorts-Hofstee, Y., Holder, M., Hoyng, C., Jones, K.J., Josifova, D., Kaitila, I., Kjaergaard, S., Kroes, Y.H., Lagerstedt, K., Lees, M., Lemerrer, M., Magnani, C., Marcelis, C., Martorell, L., Mathieu, M., McEntagart, M., Mendicino, A., Morton, J., Orazio, G., Paquis, V., Reish, O., Simola, K.O., Smithson, S.F., Temple, K.I., Van Aken, E., Van Bever, Y., van den Ende, J., Van Hagen, J.M., Zelante, L., Zordania, R., De Paepe, A., Leroy, B.P., De Buyzere, M., Coucke, P.J., Mortier, G.R., 2010. Stickler syndrome caused by COL2A1 mutations: genotype–phenotype correlation in a series of 100 patients. Eur. J. Hum. Genet. 18, 872–880.

Johnson, S.L., Weston, J.A., 1995. Temperature-sensitive mutations that cause stage-specific defects in zebrafish fin regeneration. Genetics 141, 1583–1595.

Kague, E., Bessling, S.L., Lee, J., Hu, G., Passos-Bueno, M.R., Fisher, S., 2010. Functionally conserved cis-regulatory elements of COL18A1 identified through zebrafish transgenesis. Dev. Biol. 337, 496–505.

Kawakami, K., Shima, A., 1999. Identification of the Tol2 transposase of the medaka fish *Oryzias latipes* that catalyzes excision of a nonautonomous Tol2 element in zebrafish *Danio rerio*. Gene 240, 239–244.

Kerney, R., Hanken, J., 2008. Gene expression reveals unique skeletal patterning in the limb of the direct-developing frog, *Eleutherodactylus coqui*. Evol. Dev. 10, 439–448.

Kerney, R., Hall, B.K., Hanken, J., 2010. Regulatory elements of *Xenopus* col2a1 drive cartilaginous gene expression in transgenic frogs. Int. J. Dev. Biol. 54, 141–150.

Kimmel, C.B., Ballard, W.W., Kimmel, S.R., Ullmann, B., Schilling, T.F., 1995. Stages of embryonic development of the zebrafish. Dev. Dyn. 203, 253–310.

Kimmel, C.B., Miller, C.T., Kruze, G., Ullmann, B., BreMiller, R.A., Larison, K.D., Snyder, H. C., 1998. The shaping of pharyngeal cartilages during early development of the zebrafish. Dev. Biol. 203, 245–263.

Kimmel, C.B., DeLaurier, A., Ullmann, B., Dowd, J., McFadden, M., 2010. Modes of developmental outgrowth and shaping of a craniofacial bone in zebrafish. PLoS One 5, e9475.

Koster, R.W., Fraser, S.E., 2001. Tracing transgene expression in living zebrafish embryos. Dev. Biol. 233, 329–346.

Kwan, K.M., Fujimoto, E., Grabher, C., Mangum, B.D., Hardy, M.E., Campbell, D.S., Parant, J.M., Yost, H.J., Kanki, J.P., Chien, C.B., 2007. The Tol2kit: a multisite gateway-based construction kit for Tol2 transposon transgenesis constructs. Dev. Dyn. 236, 3088–3099.

Lawson, N.D., Weinstein, B.M., 2002. *In vivo* imaging of embryonic vascular development using transgenic zebrafish. Dev. Biol. 248, 307–318.

LeClair, E.E., Mui, S.R., Huang, A., Topczewska, J.M., Topczewski, J., 2009. Craniofacial skeletal defects of adult zebrafish Glypican 4 (knypek) mutants. Dev. Dyn. 238, 2550–2563.

McAlinden, A., Majava, M., Bishop, P.N., Perveen, R., Black, G.C., Pierpont, M.E., Ala-Kokko, L., Mannikko, M., 2008. Missense and nonsense mutations in the alternatively-spliced exon 2 of COL2A1 cause the ocular variant of Stickler syndrome. Hum. Mutat 29, 83–90.

Miyamoto, Y., Nakashima, E., Hiraoka, H., Ohashi, H., Ikegawa, S., 2005. A type II collagen mutation also results in oto-spondylo-megaepiphyseal dysplasia. Hum. Genet. 118, 175–178.

Morvan-Dubois, G., Le Guellec, D., Garrone, R., Zylberberg, L., Bonnaud, L., 2003. Phylogenetic analysis of vertebrate fibrillar collagen locates the position of zebrafish alpha3(I) and suggests an evolutionary link between collagen alpha chains and hox clusters. J. Mol. Evol. 57, 501–514.

Ng, L.J., Wheatley, S., Muscat, G.E., Conway-Campbell, J., Bowles, J., Wright, E., Bell, D.M., Tam, P.P., Cheah, K.S., Koopman, P., 1997. SOX9 binds DNA, activates transcription, and coexpresses with type II collagen during chondrogenesis in the mouse. Dev. Biol. 183, 108–121.

Niu, M.C., Twitty, V.C., 1953. The differentiation of gastrula ectoderm in medium conditioned by axial mesoderm. Proc. Natl. Acad. Sci. U. S. A. 39, 985–989.

Ota, K.G., Kuratani, S., 2010. Expression pattern of two collagen type 2 alpha1 genes in the Japanese inshore hagfish (*Eptatretus burgeri*) with special reference to the evolution of cartilaginous tissue. J. Exp. Zool. B Mol. Dev. Evol. 314, 157–165.

Parichy, D.M., Elizondo, M.R., Mills, M.G., Gordon, T.N., Engeszer, R.E., 2009. Normal table of postembryonic zebrafish development: staging by externally visible anatomy of the living fish. Dev. Dyn. 238, 2975–3015.

Prockop, D.J., Kivirikko, K.I., 1995. Collagens: molecular biology, diseases, and potentials for therapy. Annu. Rev. Biochem. 64, 403–434.

Punnamoottil, B., Herrmann, C., Pascual-Anaya, J., D'Aniello, S., Garcia-Fernandez, J., Akalin, A., Becker, T.S., Rinkwitz, S., 2010. Cis-regulatory characterization of sequence conservation surrounding the Hox4 genes. Dev. Biol. 340, 269–282.

Renn, J., Winkler, C., Schartl, M., Fischer, R., Goerlich, R., 2006. Zebrafish and medaka as models for bone research including implications regarding space-related issues. Protoplasma 229, 209–214.

Sandberg, M., Vuorio, E., 1987. Localization of types I, II, and III collagen mRNAs in developing human skeletal tissues by *in situ* hybridization. J. Cell Biol. 104, 1077–1084.

Scheer, N., Campos-Ortega, J.A., 1999. Use of the Gal4-UAS technique for targeted gene expression in the zebrafish. Mech. Dev. 80, 153–158.

Schilling, T.F., 2002. The morphology of larval and adult zebrafish. In: Nusslein-Volhard, C., Dahm, R. (Eds.), Zebrafish: A Practical Approach. Oxford University Press, Oxford, UK, pp. 59–94.

Schilling, T.F., Kimmel, C.B., 1997. Musculoskeletal patterning in the pharyngeal segments of the zebrafish embryo. Development 124, 2945–2960.

Seghatoleslami, M.R., Lichtler, A.C., Upholt, W.B., Kosher, R.A., Clark, S.H., Mack, K., Rowe, D.W., 1995. Differential regulation of COL2A1 expression in developing and mature chondrocytes. Matrix Biol. 14, 753–764.

Sisson, B.E., Topczewski, J., 2009. Expression of five frizzleds during zebrafish craniofacial development. Gene Expr. Patterns 9, 520–527.

Smale, S.T., Kadonaga, J.T., 2003. The RNA polymerase II core promoter. Annu. Rev. Biochem. 72, 449–479.

Spranger, J., Winterpacht, A., Zabel, B., 1994. The type II collagenopathies: a spectrum of chondrodysplasias. Eur. J. Pediatr. 153, 56–65.

Thisse, C.T.B., 2000. High resolution whole-mount *in situ* hybridization, In: Westerfield, M. (Ed.), The Zebrafish Book. A Guide for the Laboratory Use of Zebrafish (*Danio rerio*), 4th ed. University of Oregon Press, Eugene, OR, USA.

Villemure, I., Stokes, I.A., 2009. Growth plate mechanics and mechanobiology. A survey of present understanding. J. Biomech. 42, 1793–1803.

Wada, H., Okuyama, M., Satoh, N., Zhang, S., 2006. Molecular evolution of fibrillar collagen in chordates, with implications for the evolution of vertebrate skeletons and chordate phylogeny. Evol. Dev. 8, 370–377.

Whitfield, T.T., Riley, B.B., Chiang, M.Y., Phillips, B., 2002. Development of the zebrafish inner ear. Dev. Dyn. 223, 427–458.

Woods, I.G., Wilson, C., Friedlander, B., Chang, P., Reyes, D.K., Nix, R., Kelly, P.D., Chu, F., Postlethwait, J.H., Talbot, W.S., 2005. The zebrafish gene map defines ancestral vertebrate chromosomes. Genome Res. 15, 1307–1314.

Yamamoto, M., Morita, R., Mizoguchi, T., Matsuo, H., Isoda, M., Ishitani, T., Chitnis, A.B., Matsumoto, K., Crump, J.G., Hozumi, K., Yonemura, S., Kawakami, K., Itoh, M., 2010. Mib-Jag1-Notch signalling regulates patterning and structural roles of the notochord by controlling cell-fate decisions. Development 137, 2527–2537.

Yan, Y.L., Hatta, K., Riggleman, B., Postlethwait, J.H., 1995. Expression of a type II collagen gene in the zebrafish embryonic axis. Dev. Dyn. 203, 363–376.

Yan, Y.L., Miller, C.T., Nissen, R.M., Singer, A., Liu, D., Kirn, A., Draper, B., Willoughby, J., Morcos, P.A., Amsterdam, A., Chung, B.C., Westerfield, M., Haffter, P., Hopkins, N., Kimmel, C., Postlethwait, J.H., 2002. A zebrafish sox9 gene required for cartilage morphogenesis. Development 129, 5065–5079.

Yan, Y.L., Willoughby, J., Liu, D., Crump, J.G., Wilson, C., Miller, C.T., Singer, A., Kimmel, C., Westerfield, M., Postlethwait, J.H., 2005. A pair of Sox: distinct and overlapping functions of zebrafish sox9 co-orthologs in craniofacial and pectoral fin development. Development 132, 1069–1083.

Zhang, G., Miyamoto, M.M., Cohn, M.J., 2006a. Lamprey type II collagen and Sox9 reveal an ancient origin of the vertebrate collagenous skeleton. Proc. Natl. Acad. Sci. U. S. A. 103, 3180–3185.

Zhang, R., Murakami, S., Coustry, F., Wang, Y., de Crombrugghe, B., 2006b. Constitutive activation of MKK6 in chondrocytes of transgenic mice inhibits proliferation and delays endochondral bone formation. Proc. Natl. Acad. Sci. U. S. A. 103, 365–370.

Zhou, G., Garofalo, S., Mukhopadhyay, K., Lefebvre, V., Smith, C.N., Eberspaecher, H., de Crombrugghe, B., 1995. A 182 bp fragment of the mouse pro alpha 1(II) collagen gene is sufficient to direct chondrocyte expression in transgenic mice. J. Cell Sci. 108 (Pt 12), 3677–3684.